

RADIATION INDUCED MOBILITY OF ALKALI  
ELECTROLIZED SYNTHETIC QUARTZ

By

KENNETH BARRY HITT

Bachelor of Science

Arkansas State University  
State University, Arkansas

1980

Submitted to the Faculty of the Graduate College  
of the Oklahoma State University  
in partial fulfillment of the requirements  
for the Degree of  
MASTER OF SCIENCE  
July, 1982

Thesis  
1982  
H676r  
Cop. 2



RADIATION INDUCED MOBILITY OF ALKALI  
ELECTROLIZED SYNTHETIC QUARTZ

Thesis Approved:

Joel J. Martin  
Thesis Adviser

L. M. Wilson

L. E. Halliberton

Norman D. Durham  
Dean of the Graduate College

#### ACKNOWLEDGMENTS

With the completion of this paper much thanks is owed to many people. Foremost among these is Dr. J. J. Martin. Dr. Martin has been an excellent friend, adviser and thesis committee chairman for which I owe him much. Also I must thank Dr. L. E. Halliburton and Dr. T. M. Wilson for being on my committee and for many helpful discussions. Also it is my pleasure to thank Dr. R. B. Bossoli and Dr. M. G. Jani for many helpful discussions of my results. Further I would like to thank Ms. Janet Sallee for the typing of this thesis.

Finally, I must thank God and my Mom and Dad for their love and support throughout my life and especially while at Oklahoma State University.

Financial support for this work was provided by the U.S. Air Force under Contract Number F19628-77-C-0171 as monitored by A. F. Armington.

## TABLE OF CONTENTS

Chapter	Page
I. INTRODUCTION. . . . .	1
Aluminum Related Defects . . . . .	3
Radiation Effects. . . . .	5
Purpose of Investigation . . . . .	7
II. EXPERIMENTAL PROCEDURE. . . . .	8
Infrared Absorption. . . . .	8
Temperature Dependent Irradiations . . . . .	10
Alkali Sweeping. . . . .	12
Error Analysis . . . . .	15
III. RESULTS AND DISCUSSION. . . . .	19
Sample SQ-B4 . . . . .	19
Sample PQ-E21. . . . .	25
IV. CONCLUSIONS . . . . .	30
REFERENCES. . . . .	31
APPENDIX A - TEMPERATURE VARIATIONS DURING IRRADIATION FOR SAMPLE SQ-B4 Na SWEEP #1. . . . .	33
APPENDIX B - TABULATION OF IRRADIATION DATA . . . . .	35

TABLE

Table	Page
I. Comparison of Alkali Sweeping Transport and the Number of Alkali Sites. . . . .	22

LIST OF FIGURES

Figure	Page
1. Schematic Diagram of the Cryostat Used in All Irradiations.	9
2. The Electrodiffusion (Sweeping) System. . . . .	13
3. Current Versus Time for a Typical Alkali Sweep With the Furnace Being Turned Off After Two Hours. . . . .	14
4. The Absorption Spectrum for the Same Sample After Irradia- tions at 200 and 300K . . . . .	16
5. The Absorption Spectrum for the Same Sample After Irradia- tions at 200 and 300K Showing the Greater Resolution Gained in Using a Template From the As-Received Unirradi- ated Sample and the Method Used in Measuring the $\text{Al-OH}^-$ Absorption Peaks. . . . .	17
6. The Growth of the $\text{Al-OH}^-$ Infrared Absorption Peaks as a Function of Irradiation Temperature for the Same Sample After Each of Two Consecutive Sodium Sweeps . . . . .	20
7. The Concentration of $\text{Al-OH}^-$ Centers as a Function of Irra- diation Temperature for Irradiations Performed on the Same Sample While in the As-Received, Sodium-Swept, and Lithium-Swept Conditions. The Concentration is Normalized to the As-Received Condition . . . . .	24
8. The Concentration of $\text{Al-OH}^-$ Centers as a Function of Irra- diation Temperature for Irradiations Performed on the Same Sample While in the Lithium-Swept (As-Received) and Sodium-Swept Conditions. The Concentration is Normal- ized to One for Each Condition. . . . .	26
9. The Growth of $\text{Al-OH}^-$ Infrared Absorption Peaks as a Func- tion of Irradiation Temperature . . . . .	27
10. The Concentration of $\text{Al-OH}^-$ Centers as a Function of Irra- diation Temperature for Irradiations Performed on the Same Sample While in the As-Received and Sodium Swept Conditions. The Concentration is Normalized to the As- Received Condition. . . . .	28

11. The Concentration of Al-OH<sup>-</sup> Centers as a Function of Irradiation Temperature for Irradiations Performed on the Same Sample While in the As-Received and Sodium Swept Conditions. The Concentration is Normalized to One for Each Condition. . . . . 29



## CHAPTER I

### INTRODUCTION

The use of quartz controlled oscillators has grown dramatically over the last few years. In today's consumer market few new electronic products lack the phrase "quartz-locked" or "quartz-tuned" in their product descriptions. Quartz has become a symbol for quality. Yet in some high precision frequency control applications, such as navigation satellites or deep-space probes where oscillators are frequently exposed to a radiation environment, quartz often fails to meet the requirements. In these circumstances quartz oscillators have a tendency to change frequency and in some cases stop oscillation. This thesis is presented as a part of the current research being conducted at Oklahoma State University aimed at understanding the underlying defects responsible for these frequency changes.

Quartz has two solid phases,  $\alpha$ (low quartz) and  $\beta$ (high quartz), with the  $\alpha$ - $\beta$  phase transition occurring at  $573^{\circ}\text{C}$ . The hexagonal  $\beta$  phase is of little technological importance. In contrast,  $\alpha$ -quartz, of trigonal symmetry, is the most frequently used material in crystal oscillators (due to its low damping and strong piezoelectric properties).  $\alpha$ -Quartz, henceforth referred to as quartz, has a melting point of  $1750^{\circ}\text{C}$ , a density of  $2.65 \times 10^3 \text{ Kg/m}^3$  and a hardness of 7 on the moh scale. It is only slightly soluble in water, but can be dissolved by hydrofluoric acid.

Quartz has an axis of threefold symmetry. This axis is referred to as the *c*, or optic axis. Along this axis are wide channels of approximately one Angstrom radius. In the plane perpendicular to *c*-axis are three equivalent axes of two-fold symmetry, 120 degrees apart called the *a*-axes. In this plane are smaller channels.

In many applications, it is convenient to describe the crystal using a Cartesian coordinate system. The recent IEEE Standard on Piezoelectricity (1) defines such a system. The Z axis is chosen parallel to the *c* axis. The X axis is chosen to lie along one of the *a* axes and the Y axis is appropriately chosen to complete the right-handed coordinate system.

Natural quartz, mined chiefly in Brazil, is used throughout the electronics industry. Yet due to quality control and production problems, natural quartz is quickly being superseded by synthetically grown. Because of the 573°C  $\alpha$ - $\beta$  structural phase transition synthetic quartz is grown using hydrothermal techniques. Commercially (2) the technique involves placing racks on which seeds are held into a pressure vessel which has quartz nutrient at its bottom. The autoclave vessel is then filled with a mineralizer solution of  $\text{Na}_2\text{CO}_3$  or NaOH in water. Usually a small quantity of LiOH is added to improve the crystal's homogeneity (3). The vessel is closed and the temperature slowly raised to the temperature range of 340 to 370°C, with an attendant pressure of approximately 2000 atmospheres. A small thermal gradient is maintained between the seeds and the nutrient to produce a thermal circulation within the solution. As the solution circulates, material is deposited on the seeds to form single crystals. Typical growth periods are from 60 to 120 days. Impurities present in the final product can come from the

starting materials, the mineralizers, the lithium salt or the pressure vessel walls. The overall impurity concentration in synthetic quartz is at least an order of magnitude lower than for natural quartz (4).

#### Aluminum Related Defects

Most of the quartz related research into radiation effects has been directed towards the presence of aluminum in the crystal. Aluminum, approximately the same size and mass as silicon, easily substitutes for silicon in the crystal lattice. With this substitution there is the need for some form of charge compensator since aluminum exists in a 3+ valence state whereas silicon exists in a 4+ state. Recent work by Halliburton et al. (5) suggests that for commercially grown material these compensators may take on only three forms, an interstitial alkali ion, an interstitial hydrogen ion, or a hole.

The defect center formed between the alkali and the aluminum, notationally represented by  $\text{Al-M}^+$  where  $\text{M}^+$  is the alkali ion, is the predominant aluminum center in the as-grown material. The alkali may be either Na or Li with the Li being in much greater quantity (6). Stress-induced motion of the alkali between equilibrium positions about the aluminum can give rise to acoustic loss peaks. Work done by King (7) and Fraser (8,9) on 5 MHz 5th overtone AT-cut quartz resonators has led to the assigning of a 50K acoustic loss peak to the  $\text{Al-Na}^+$  center. The 50K Na acoustic loss peak and the related dielectric loss are the only direct evidence of the  $\text{Al-Na}^+$  center (10). In AT-cut crystals no acoustic loss peaks can be assigned to  $\text{Al-Li}^+$  center (11). At present no direct means of monitoring the  $\text{Al-Li}^+$  center is known.

Upon irradiation at room temperature there is the conversion of

$\text{Al-M}^+$  centers into relatively large quantities of aluminum-OH centers. The aluminum-hydroxide center, notationally represented as  $\text{Al-OH}^-$ , is believed to be produced as interstitial alkali ions are moved from the aluminum site followed by the simultaneous movement of hydrogen from unknown centers in the crystal to the aluminum site. The proton then bonds with an adjacent oxygen to form the  $\text{Al-OH}^-$  center. The resulting  $\text{Al-OH}^-$  center is stable at room temperature yet it can be completely removed by anneals at temperatures above  $400^\circ\text{C}$ , for irradiated samples (12). Kats (13) has associated this defect center with infrared absorption peaks at 3367 and  $3306\text{ cm}^{-1}$  from work he did on deuterium electro-lized crystals. Additional work done by Brown and Kahan (14) and Halliburton et al. (5) have confirmed Kats' assignment.

Also upon room temperature irradiation there is the production of aluminum-hole centers. This center, denoted Al-hole, was first reported by Griffith, Owen and Ward (15). It is both EPR and optically (16) active. The aluminum-hole center is also responsible for acoustic loss peaks at 25, 100 and 135K (10,11,17). O'Brien (18) described the center as a hole trapped in a non-bonding 2p orbital of the oxygen bridging between the aluminum and a silicon. This center may come about when the irradiation, electron or x-ray, forms electron-hole pairs within the lattice. If sufficient electron traps are available, a hole can be trapped at one of the non-bonding p-orbitals. A comprehensive review of the aluminum hole center as well as all the aluminum related centers is given by Weil (19).

The electrodiffusion or sweeping process, initially developed by King (7), has greatly helped in the identification of aluminum-compensator defects. The process consists of applying an electric field across

the crystal, parallel to the crystal's c-axis, while the crystal is held at elevated temperatures. Because of quartz's large c-axis channels, the cation interstitials, which are sitting in the channels, are transported away from the aluminum site towards the negative electrode. Simultaneously other cations, introduced at the positive electrode, are transported through the crystal coming to rest at the aluminum sites. The technique thus allows great freedom in selectively doping the crystal with the particular compensator (i.e.  $H^+$ ,  $Li^+$ ,  $Na^+$ ,  $D^+$ , etc.) to be studied.

#### Radiation Effects

The basic radiation response mechanism in  $\alpha$ -quartz is the radiation-induced mobility of interstitial ions. When a crystal is irradiated, cation interstitials are freed from their aluminum traps and diffuse away from the aluminum site. Simultaneously other cations move to the aluminum site. Because of the changes in the local crystalline field, due to the exchange, there are attendant changes in the crystal's mechanical property's (i.e. quality factor, resonance frequency, etc.). In a parallel set of studies on the aluminum-compensator defects, Sibley et al. (12), Markes and Halliburton (20), and Doherty and Martin (21) have presented a clear picture of the mechanics of these radiation-induced exchanges.

Sibley et al. (12) in their study of the effects of radiation on the  $Al-OH^-$  center found that hydrogen is mobile under irradiation down to at least 15K. They found that the  $Al-OH^-$  center was produced only if the sample was held at temperatures greater than approximately 200K during the irradiation. They suggested that only at temperatures

greater than approximately 200K would the interstitial alkalis move away from the aluminum site in the presence of a radiation field. A subsequent irradiation at 77K suppressed the  $\text{Al-OH}^-$ ; however, it recovered upon warming to room temperature. In unswept quartz they found that the radiation-produced  $\text{Al-OH}^-$  center anneals out at approximately  $400^\circ\text{C}$ .

Markes and Halliburton (20) studied irradiation effects on the Al-hole center. In their work they found that the production of Al-hole centers was greatly enhanced when, for example, a room temperature irradiation was followed by a 77K irradiation. Further they found, using ESR techniques, that hydrogen is mobile at 77K and that the irradiation produced Al-hole centers, in unswept samples, can be removed by anneals at temperatures around  $270^\circ\text{C}$ . Also they found, using the irradiation technique described above, that the production of Al-hole centers in unswept quartz is highly temperature dependent. Below 200K, irradiations produce only relatively small numbers of Al-hole centers, yet above this temperature the production is large. At around 300K they found that the radiation production of hole centers was essentially saturated.

Doherty and Martin (21) studied the effects of radiation on the  $\text{Al-Na}^+$  center. In their work they monitored the 50K acoustic loss peak, on 5 MHz 5th overtone AT-cut resonators, after a series of irradiations over the temperature range 77 to 300K. They found that the  $\text{Al-Na}^+$  center was stable under irradiation for temperatures below 200K. Above this temperature, irradiation caused the loss peak to quickly decrease. The removal was essentially complete by 300K.

In each of these papers attempts were made to correlate their combined results. The general picture is as follows. When a quartz crystal

is irradiated at temperatures above 200K the interstitial alkali ions at the aluminum site are replaced by protons (ionized hydrogen) or holes on an adjacent oxygen. Since the alkalis, that moved away, are only mobile at temperatures above 200K, while hydrogen is mobile at all temperatures, a subsequent irradiation at 77K will cause the hydrogen to become mobile. The hydrogen moves away from aluminum site and is replaced by a hole. When the sample is annealed to temperatures above 400°C the holes and the hydrogen ions present at the aluminum sites will move away and the alkalis will return as had been previously reported (7,22).

#### Purpose of Investigation

As-received synthetic quartz, used by Doherty and Martin (21), Markes and Halliburton (20) and Sibley et al. (12), contains both  $\text{Na}^+$  and  $\text{Li}^+$  as alkali compensators at the aluminum site. Unfortunately no direct means is known for monitoring  $\text{Li}^+$ . Further  $\text{Li}^+$  is believed to be the predominant alkali. As a consequence, the monitoring of the  $\text{Al-Na}^+$  center under irradiation may not correctly reflect the actual radiation-induced mobility of alkali interstitials in the crystal. The purpose of the study presented here is to determine whether or not the alkali present at the aluminum site will effect the radiation-induced mobility. More specifically will the onset of mobility for the crystal be different for purely  $\text{Na}^+$  or  $\text{Li}^+$ -aluminum compensated crystals? The means chosen here to monitor any difference is the growth of the  $\text{Al-OH}^-$  bands as a function of irradiation temperature.

## CHAPTER II

### EXPERIMENTAL PROCEDURE

High quality, commercially grown, synthetic quartz was used exclusively in this study. Z-plates, rectangular plates perpendicular to the crystallographic z-axis, were cut from pure z-growth, lumbered bars purchased from Sawyer Research Products (23) and Toyo Communications Incorporated (24). The plates, which were approximately 3mm thick, 15mm long and 10mm wide, were then cleaned and polished to an optical finish. The samples were identified according to the notation of Markes and Halliburton (20). Using this notation a sample was identified according to grade, Premium Q (PQ) or Supreme Q (SQ), according to the bar, A, B, C, etc. and according to cut 1, 2, 3, etc. For example, sample SQ-B4 would be the 4th sample cut from the Bth Supreme Q bar.

Samples were mounted in the temperature controlled cryostat shown schematically in Figure 1. The sample was clamped in a copper holder attached to the cryostat's cold finger. A chromel-alumel thermocouple was soldered to the holder. The rotatable cryostat tail had three  $\text{CaF}_2$  optical windows and one aluminum irradiation window. The irradiation window was approximately 0.13 mm thick. The sample enclosure was evacuated to a pressure of about  $5 \times 10^{-6}$  torr.

### Infrared Absorption

All absorption measurements were made using a Beckman Model 4240



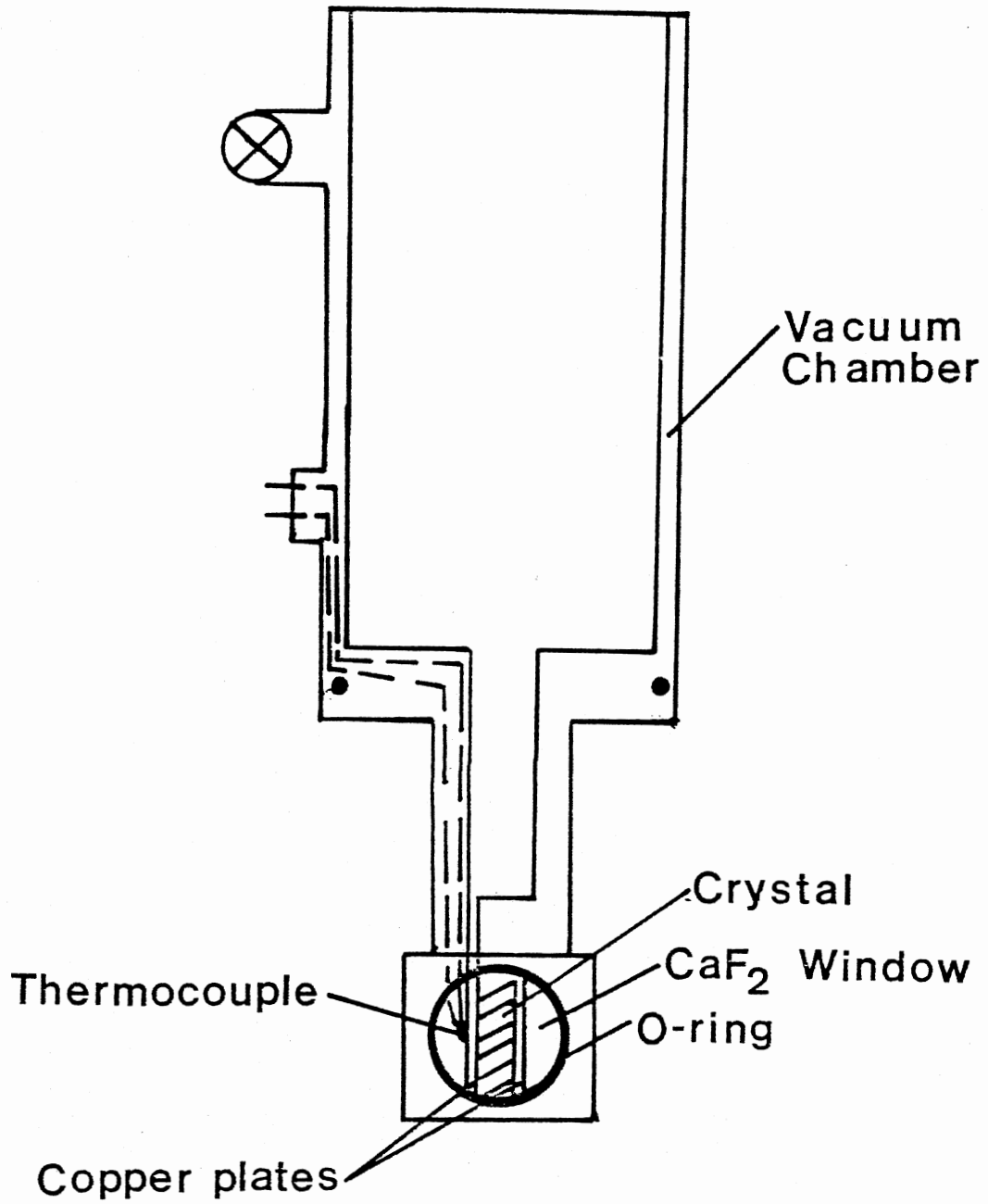


Figure 1. Schematic Diagram of the Cryostat Used in all Irradiations

Infrared Spectrophotometer. The sample was enclosed in the cryostat with windows rotated so that light would pass through the sample. Unpolarized light was used. The electric field vector was then perpendicular to the crystal's z-axis. This arrangement was chosen so as to avoid polarization effects as described by Lipson et al. (25). The crystal was maintained at approximately 80K during measurements, as the absorption is highly temperature dependent (26). Since the infrared absorption of high quality quartz is relatively low, a Heath/Schlumberger Model SR-204 chart recorder was set up to record the data on the expanded range of 0-0.2 absorbance. The chart drive of the Heath recorder was locked to the Beckman scan drive. The absorption was measured over the range 4000-3000  $\text{cm}^{-1}$ . The heights of the peaks at 3306 and 3367  $\text{cm}^{-1}$  were recorded and their absorption coefficients calculated from the equation,

$$\alpha = \frac{23.03 H_{\text{peak}}}{t} \quad (1)$$

where  $\alpha$  is the absorption coefficient, in  $\text{cm}^{-1}$ ,  $H_{\text{peak}}$  is the height of the absorption peak and  $t$  is the sample thickness in mm.

#### Temperature Dependent Irradiations

All irradiations were made with a Van de Graaff accelerator. The irradiations were done with 1.7 MeV electrons for a total of 4 minutes. Typical doses were approximately 2000  $\text{J/cm}^3$  ( $\sim 10^8$  rads). Since the thickness of the samples were about 3mm and the penetration depth of electrons in quartz is about 2mm, samples were irradiated on both sides for 2 minutes each. The irradiations were carried out through the

cryostat's irradiation port with the sample located 15 cm from the Van de Graaff's aluminum foil window.

Temperature measurements were made via the chromel-alumel thermocouple which was attached to the cryostat's copper sample holder. The thermocouple wires were brought out of the cryostat and were connected to an Omega Model MCJ Electronic Ice Point, which served as a temperature reference. The temperature reference was connected outside the radiation area to a Hewlett Packard Model 3465B Multimeter, via a 15 meter long coaxial cable. The multimeter's display was visually monitored during the irradiation with initial and final voltages recorded. The National Bureau of Standards thermocouple tables were used to convert the measured voltages into temperatures. The assigned temperature for data plots and calculations was the arithmetic mean of the initial and final temperatures for the irradiation.

Irradiations were made at progressively higher temperatures starting at 77K. The temperatures were achieved by the process described below. For irradiation temperatures of 77K, 196K, and 273K, liquid nitrogen, dry ice and water ice were used respectfully. During these irradiations the sample temperature would rise only a few degrees as indicated by the thermocouple readings. The sample was allowed to cool back to the fixed point, determined by the fluid, before the second side was irradiated. For irradiations at temperatures other than these fixed points, a small quantity of the appropriate cryogenic fluid was placed in the cryostat's reservoir until the sample cooled to the desired temperature. Then the fluid was poured out and the irradiation for one side of the sample was carried out. A temperature rise of approximately 10K was observed during the irradiation. The sample was then cooled back to the starting temperature for the second irradiation. After the second irradiation, liquid nitrogen was placed in the cryostat so that

the optical measurements could be made at 80K.

### Alkali Sweeping

Alkali sweeping or electrodiffusion, in which selected alkali ions are diffused into quartz, replacing holes, hydrogen or other alkalis, took place in the system shown in Figure 2. The sample is clamped between graphite electrodes which were connected to a voltage source. The electrodes were inside the end of a silica tube, which was surrounded, at that end, by a high temperature furnace. The sample has gold vapor deposited electrodes on its faces with an appropriate salt film being previously vapor deposited on one of its faces. The orientation of the sample can be seen to be such that alkali ions supplied by the salt, will be transported through the crystal.

The procedure consisted of first evacuating the silica tube to an eventual pressure of approximately  $5 \times 10^{-6}$  torr. Upon reaching this pressure, the furnace was turned on and the sample temperature raised to approximately  $470^{\circ}\text{C}$ . At this temperature an electric field of approximately 1-5 volts/cm was applied. The current was recorded as a function of time using a Heath/Schlumberger Model SR-204 chart recorder. Figure 3 shows a typical current versus time curve. The nearly constant current up till the furnace was turned off (after approximately 2 hours) is believed to be due to the salt source-film continually supplying alkalis to the crystal (10). When the furnace is turned off the thermally activated ionic mobility decreases rapidly and the current quickly decreases to near zero. To prevent the cations which had been swept out of the sample from diffusing back, the electric field was maintained until the sample had cooled below  $150^{\circ}\text{C}$ . Upon reaching room temperature the sample was removed from the system, appropriately cleaned of films

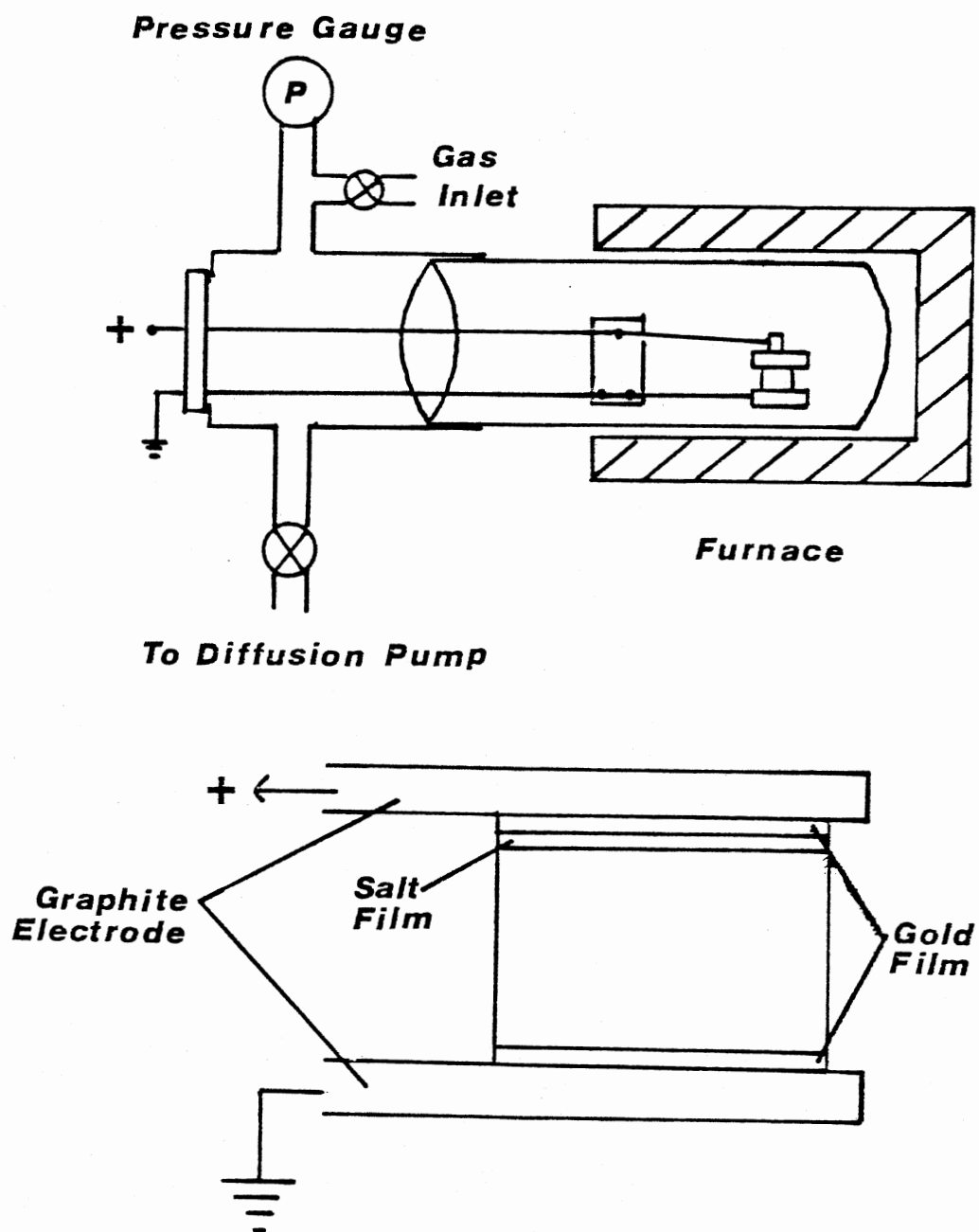


Figure 2. The Electrodiffusion (Sweeping) System

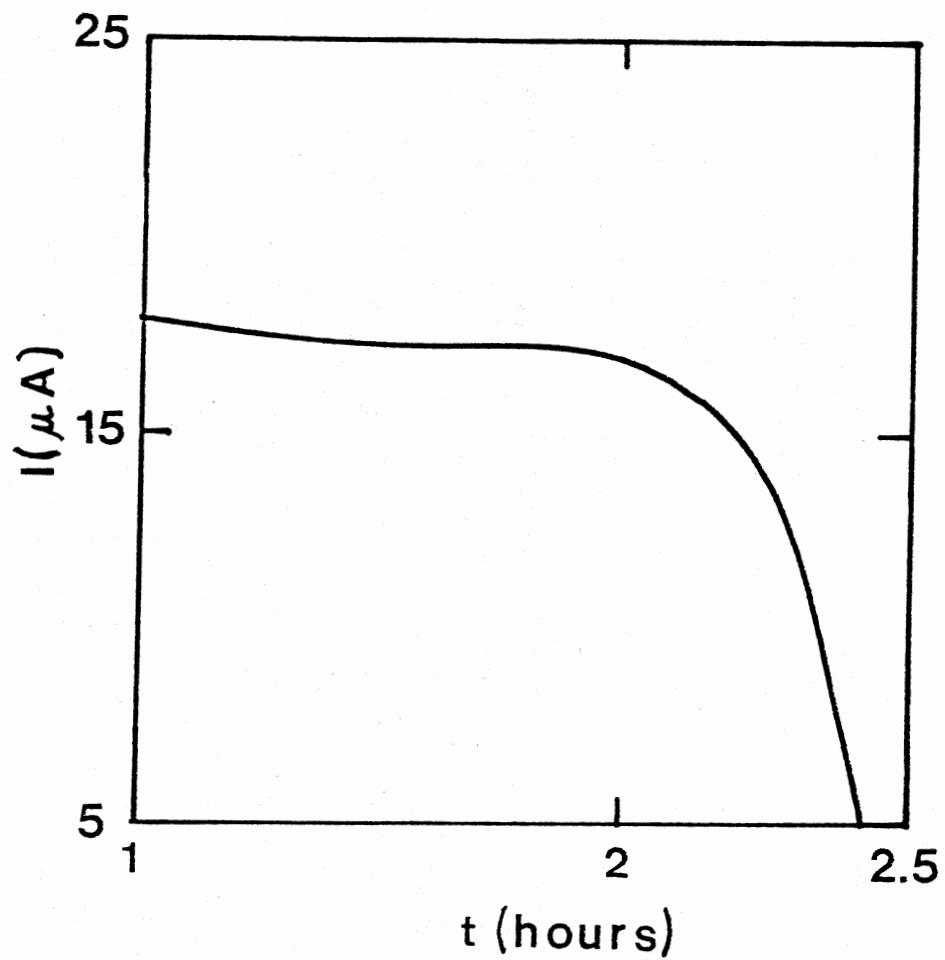


Figure 3. Current Versus Time for a Typical Alkali Sweep With the Furnace Being Turned Off After Two Hours

and mounted in the cryostat.

#### Error Analysis

The most notable error in these experiments was that produced in the temperature measurements during irradiations. Appendix A shows the temperature measurements made for a particular sample. At temperatures where a standard coolant was kept in the cryostat the temperature varied only 3 to 4 degrees. Yet at temperatures between standards the irradiations produced warming of between 4 and 10 degrees. Since most irradiations were done at these intermediate temperatures the assigned temperature for an irradiation is expected to be good to  $\pm 5\text{K}$ . In addition, since the thermocouple was not calibrated a systematic error of approximately  $\pm 2\text{K}$  may be present. This systematic error will not effect the relation of one run to another.

Further uncertainties occurred in the optical measurements. Figure 4 shows a typical spectra taken after 200 and 300K irradiations, for the same sample. In these recordings the  $3367\text{ cm}^{-1}$  peaks have a fairly well defined base line. In contrast, the  $3306\text{ cm}^{-1}$  peaks sit on the shoulder of a broad intrinsic peak centered at  $3300\text{ cm}^{-1}$ . In order to estimate the absorption of the  $3306\text{ cm}^{-1}$  band, from the as-received, unirradiated spectrum's graph a template for the absorption band at  $3300\text{ cm}^{-1}$  was cut out and laid over this area of the recordings for subsequent irradiations. Figure 5 shows the same graphs after this has been done and the way the peak heights were measured. Using this technique, the absorption at  $3306\text{ cm}^{-1}$  is now quite evident and the expected error in absorption height measurements is estimated to be around 5% for the large absorption peaks.

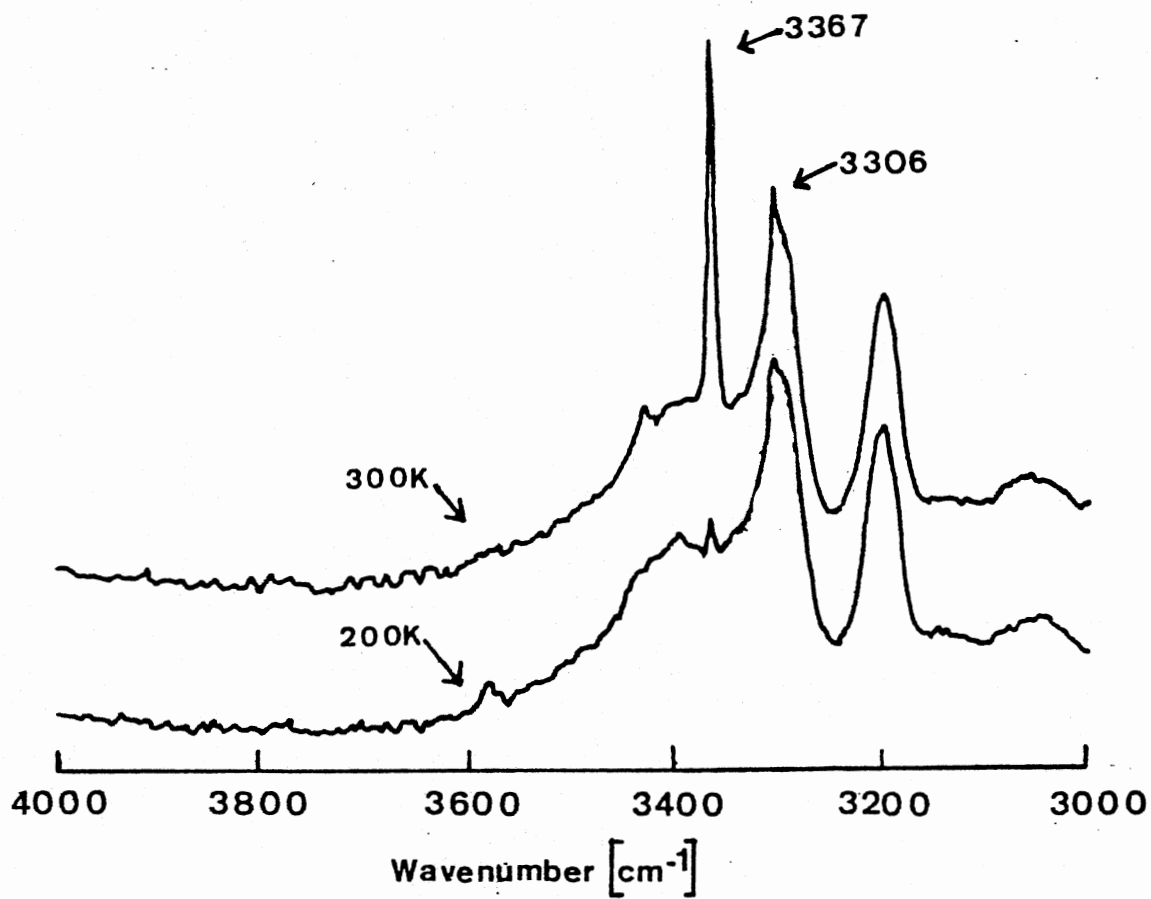


Figure 4. The Absorption Spectrum for the Same Sample After Irradiations at 200 and 300K



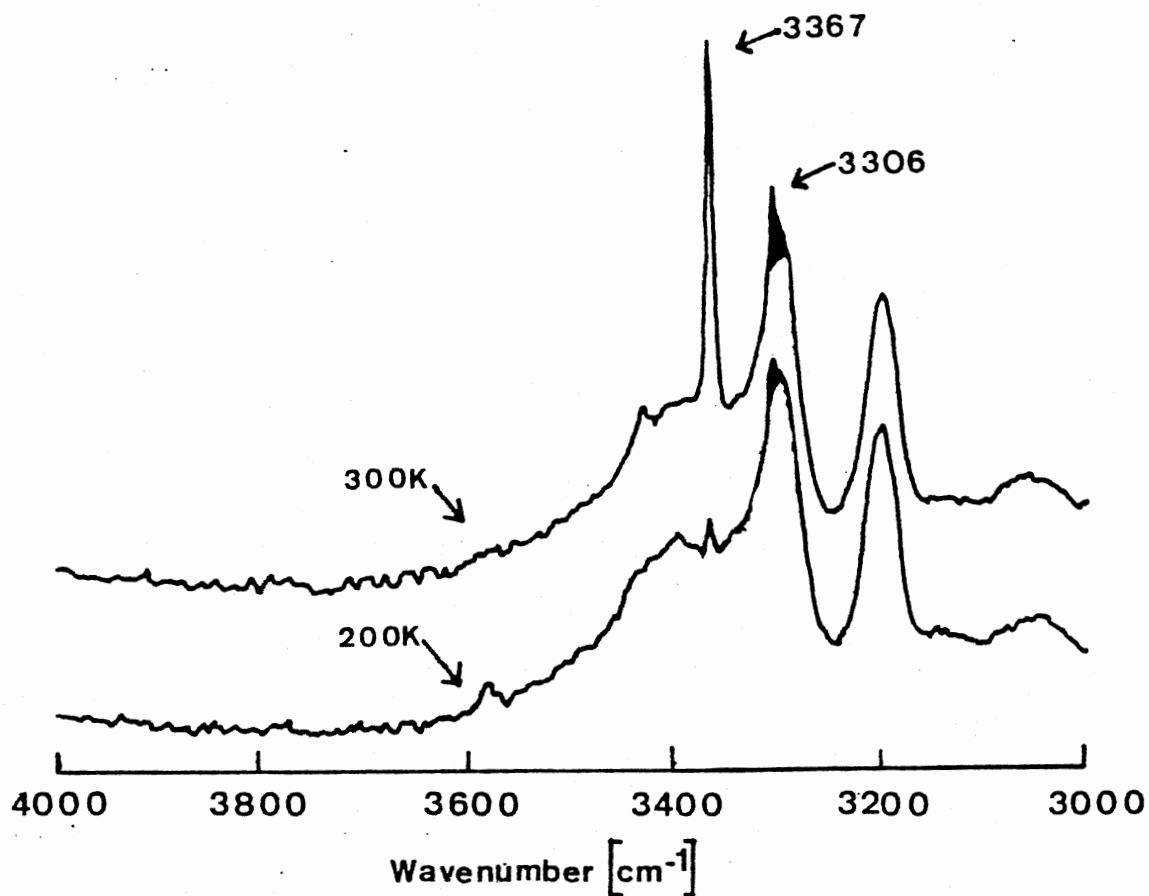


Figure 5. The Absorption Spectrum for the Same Sample After Irradiations at 200 and 300K Showing the Greater Resolution Gained in Using a Template From the As-Received Unirradiated Sample and the Method Used in Measuring the Al-OH<sup>-</sup> Absorption Peaks

Still further error occurred as a result of small fluctuations in the dose. Although attempts were made to fix the dose, variation occurred in the crystal's placement, in the electron energy and in the irradiation time. The crystal's placement with respect to the Van de Graaff window was fixed to within 5 mm. The electron energy was accurate to within 0.2 MeV and the time of irradiation to within 1 second. Yet the corresponding additive error is expected to be approximately 10%.

The uncertainties in the experiment are summarized as follows. The irradiation temperature is within  $\pm 5K$ . The repeatability of the irradiation dose is expected to be within 10% and the absorption band heights were within 5% for the larger bands.

## CHAPTER III

### RESULTS AND DISCUSSION

In this study irradiations and electrodiffusion were performed on two different samples from different sources. Work on sample SQ-B4 (Toyo Supreme grade quartz) forms the main basis of this thesis. The work was repeated on sample PQ-E21 (Sawyer Premium grade quartz) to verify the results on SQ-B4. On both samples irradiations were carried out starting at 77K and proceeding to above 300K. In general, since the results of interest occur above 200K, only data above this temperature is presented, although irradiations were performed below 200K.

#### Sample SQ-B4

Irradiations were performed on this sample while in the as-received condition, after a 1st  $\text{Na}^+$  sweep, after a 2nd  $\text{Na}^+$  sweep and after a  $\text{Li}^+$  sweep. Figure 6 shows the growth of the 3306 and 3367  $\text{cm}^{-1}$  bands as a function of irradiation temperature, after each of two  $\text{Na}^+$  sweeps. The two bands grow almost linearly, at the same rate, over the temperature range 200 to 250K. Above 250K the 3367 band grows quickly reaching saturation around 320K. In contrast, above 250K the 3306 band decreases becoming essentially constant around 280K. This growth pattern, which, in this study, has been found to be true for as-received,  $\text{Na}^+$  and  $\text{Li}^+$  swept samples, was first reported by Sibley et al. (12). Sibley et al., whose work was done on as-received samples only, attributed the pattern

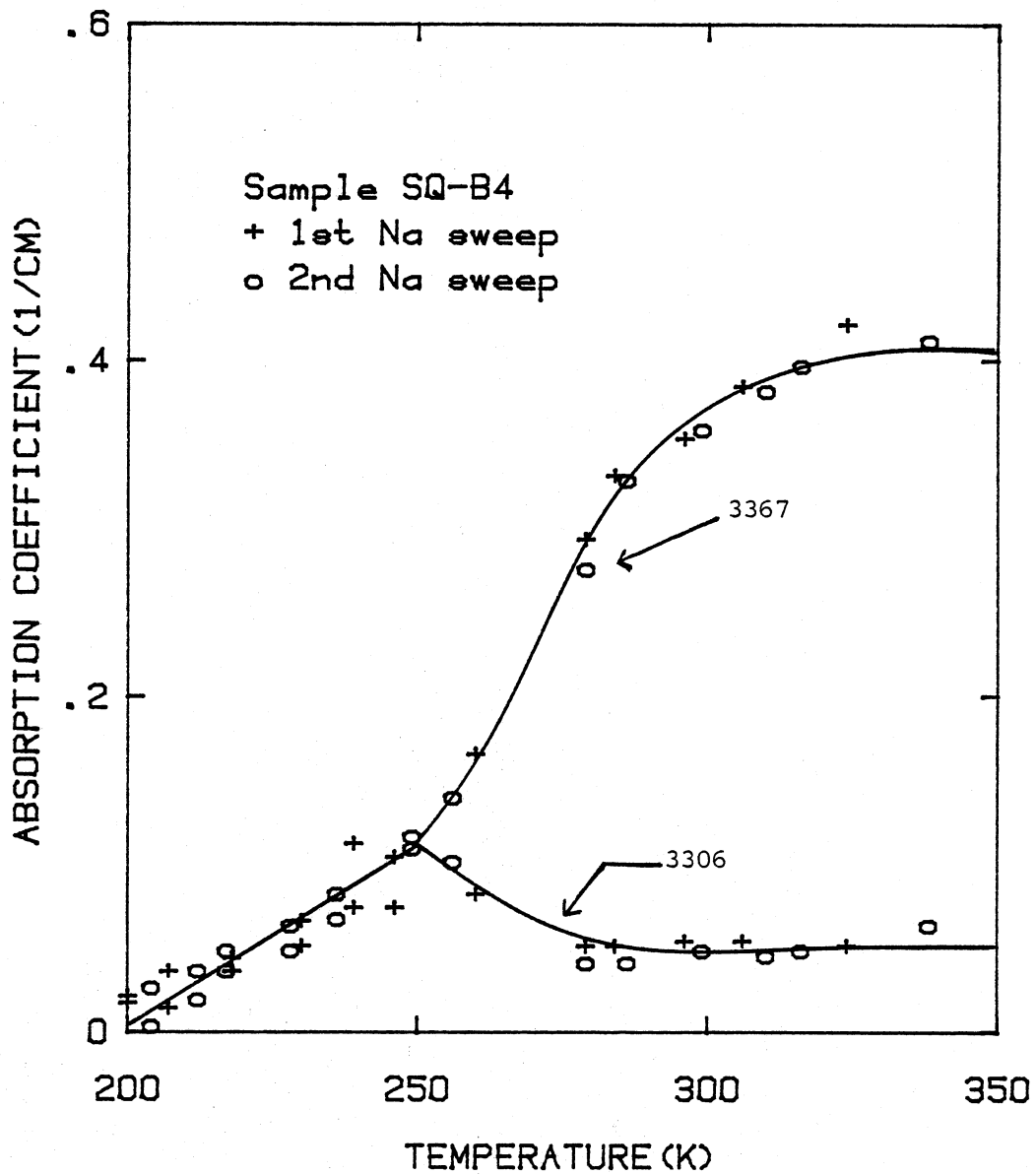


Figure 6. The Growth of the  $\text{Al-OH}^-$  Infrared Absorption Peaks as a Function of Irradiation Temperature for the Same Sample After Each of Two Consecutive Sodium Sweeps

to a phonon-assisted process occurring between  $\text{OH}^-$  ions existing at two different, but closely related, symmetry sites. Figure 6 also gives a good indication of the reproducibility of this experiment. The data presented is for sets of irradiations which were performed after each of two successive sodium sweeps. As can be seen the curve is the same for each sweep.

Table I describes the electrodiffusion data for the samples used in this experiment. In this table  $N_H$  is the concentration of  $\text{OH}^-$  ions (number/cm<sup>3</sup>) in the sample. The value given was computed from the equation

$$N_H = 2.16 \times 10^{16} H \alpha_m . \quad (1)$$

This equation, originally presented by Kats (12), gives the concentration of  $\text{OH}^-$  ions ( $N_H$ ) in terms of the half-width  $H(\text{cm}^{-1})$  of the  $\text{OH}^-$  bands and the bands maximum absorption coefficient  $\alpha_m(\text{cm}^{-1})$ . For the computation, the half-widths were taken to be  $7.6 \text{ cm}^{-1}$ , for both bands, and the maximum absorption coefficient was that observed for the highest temperature irradiation performed, on the as-received sample. Since in irradiations at room temperature the number of Al-hole centers produced may be as high as the number of Al- $\text{OH}^-$  centers produced (20) the Al- $\text{OH}^-$  center concentration has been doubled in order to estimate the total aluminum content.  $N_{Al}$  is the total number of Al- $\text{OH}^-$  centers in the sample, computed by multiplying  $N_H$  by the volume.  $N_{\text{TRANS}}$  is the number of alkali ions transported through the crystal during the sweep. This number was computed from the constant part of the current versus time graph, where it was assumed that the salt film, deposited on the crystal, was constantly supplying alkali ions which were replacing the ions

TABLE I

COMPARISON OF ALKALI SWEEPING TRANSPORT AND THE  
NUMBER OF ALKALI SITES

Sample	$N_H (10^{16} \text{ cm}^{-3})$	Sweep	$N_{Al} (X 10^{16})$	$N_{Trans} (X 10^{16})$	$N_{Trans}/N_{Al}$
SQ-B4	18.3	1st Na	15	15	1
	18.3	2nd Na		140	9.3
	18.3	Li		22	1.5
PQ-E21	12.6	Na	4.8	5.6	1.2

of the aluminum site. The ratio,  $N_{\text{Trans}}/N_{\text{Al}}$ , shows that for each sweep the number of alkalis transported was at least equal to the number of aluminum sites. Also the table shows that this number transported is essentially enough to fill the aluminum sites. This statement is drawn from this table because for the two  $\text{Na}^+$  sweeps there is a large difference in the number of alkali ions transported yet as has already been shown the irradiation curves are the same.

Figure 7 shows the concentration of  $\text{OH}^-$  ions as a function of irradiation temperature. The data presented was taken for first, the as-received condition then for two  $\text{Na}^+$  sweeps (only data for one  $\text{Na}^+$  sweep is shown to reduce cluttering) and then for a  $\text{Li}^+$  sweep, in that order. The curves for the as-received and the  $\text{Li}^+$  sweep appear to be the same. This situation is not too surprising for the current belief is that  $\text{Li}^+$  is the predominant alkali in quartz (6). Further the graph shows that the curve for the  $\text{Na}^+$  sweeps is shifted to a higher temperature. This shift is of approximately 15K taking into account the  $\pm 5\text{K}$  error in the temperature measurements. The shift is believed to be due to the difference in the mass and ionic radius of the alkalis. Na has approximately three times the mass of Li and its ionic radius is about 1.5 times that of Li. It then seems reasonable that Li should be more easily moved away from the aluminum site. Also from the graph it should be noted that there appears to be a saturation level difference between the as-received ( $\text{Li}^+$  swept) condition and that for a  $\text{Na}^+$  sweep. This situation, from which it might be concluded that more hole centers are produced, is not yet understood. Yet the order in which the irradiations were performed, as received, two  $\text{Na}^+$  sweeps and then a  $\text{Li}^+$  sweep, indicates that this situation can be reversed.

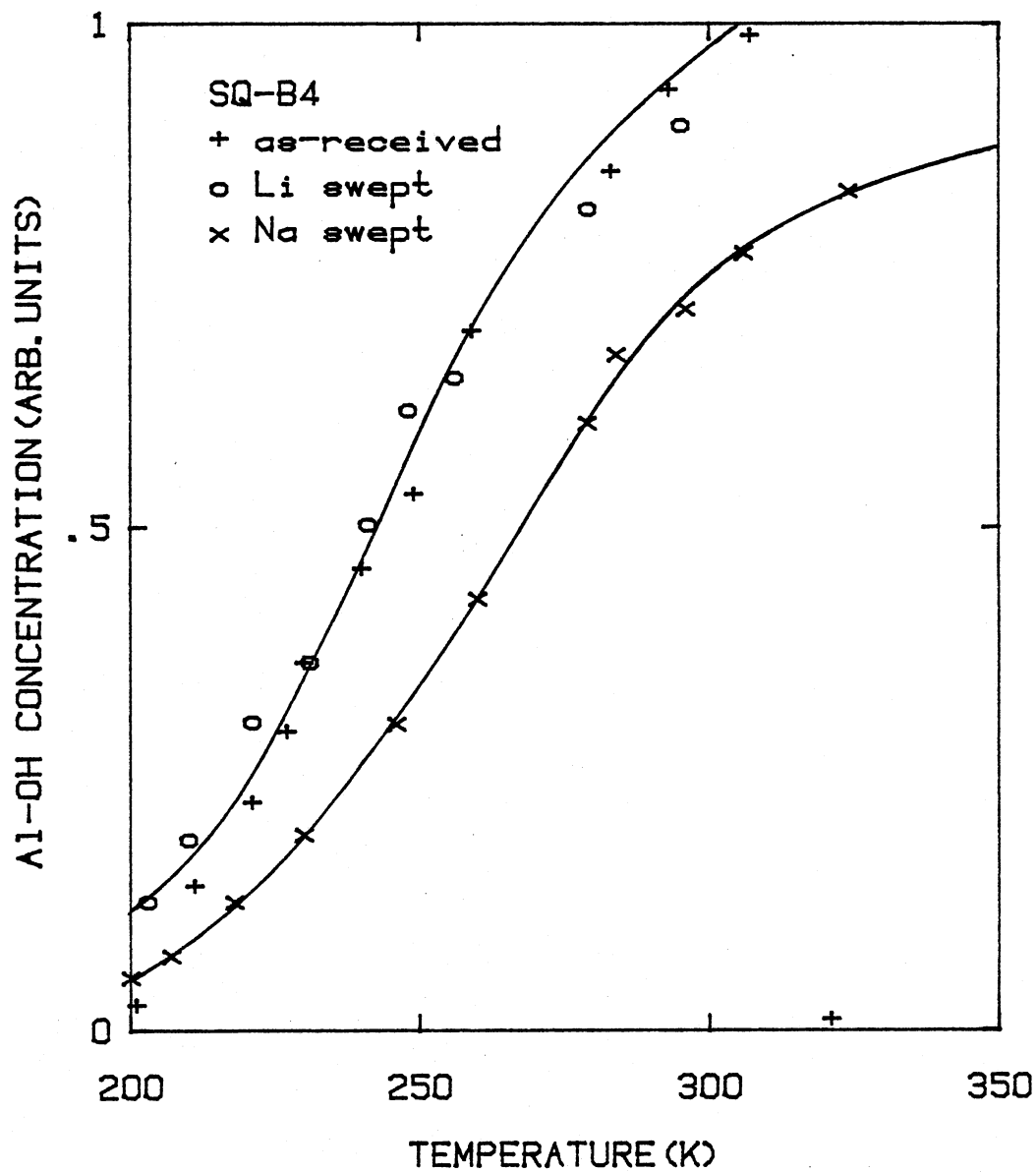


Figure 7. The Concentration of Al-OH<sup>-</sup> Centers as a Function of Irradiation Temperature for Irradiations Performed on the Same Sample While in the As-Received, Sodium-Swept, and Lithium-Swept Conditions. The Concentration is Normalized to the As-Received Condition



In the light of the difference in the saturation levels shown, the level difference might be construed as being the cause of shift upward in temperature for the Na sweeps. To address this question, Figure 8 shows the data for the  $\text{Li}^+$  sweep (as-received) and the  $\text{Na}^+$  sweep normalized to the same saturation level. Given that the normalized curves now saturate at the same level there still appears to be an upward temperature shift for the  $\text{Na}^+$ -swept condition. This shift again is of approximately 15K.

#### Sample PQ-E21

For this sample, irradiations were performed while the sample was in the as-received condition and after a  $\text{Na}^+$  sweep. Figure 9 shows the growth of the  $\text{OH}^-$  bands as a function of irradiation temperature. The graph shows that the growth pattern described by Sibley et al. (11) and presented for various sweeps in this paper, still occurs. For this sample, the pattern, shown for the as-received condition only, also was repeated for the  $\text{Na}^+$  sweep performed. Figure 10 shows the concentration of  $\text{OH}^-$  ions as a function of irradiation temperature. As was the case for SQ-B4, the curve for the  $\text{Na}^+$ -swept condition is shifted approximately 15K higher in temperature than the as-received ( $\text{Li}^+$ -swept) condition. Again a large saturation level difference occurs. In Figure 11, the saturation difference is, as before, shown not to be the cause of the shift.

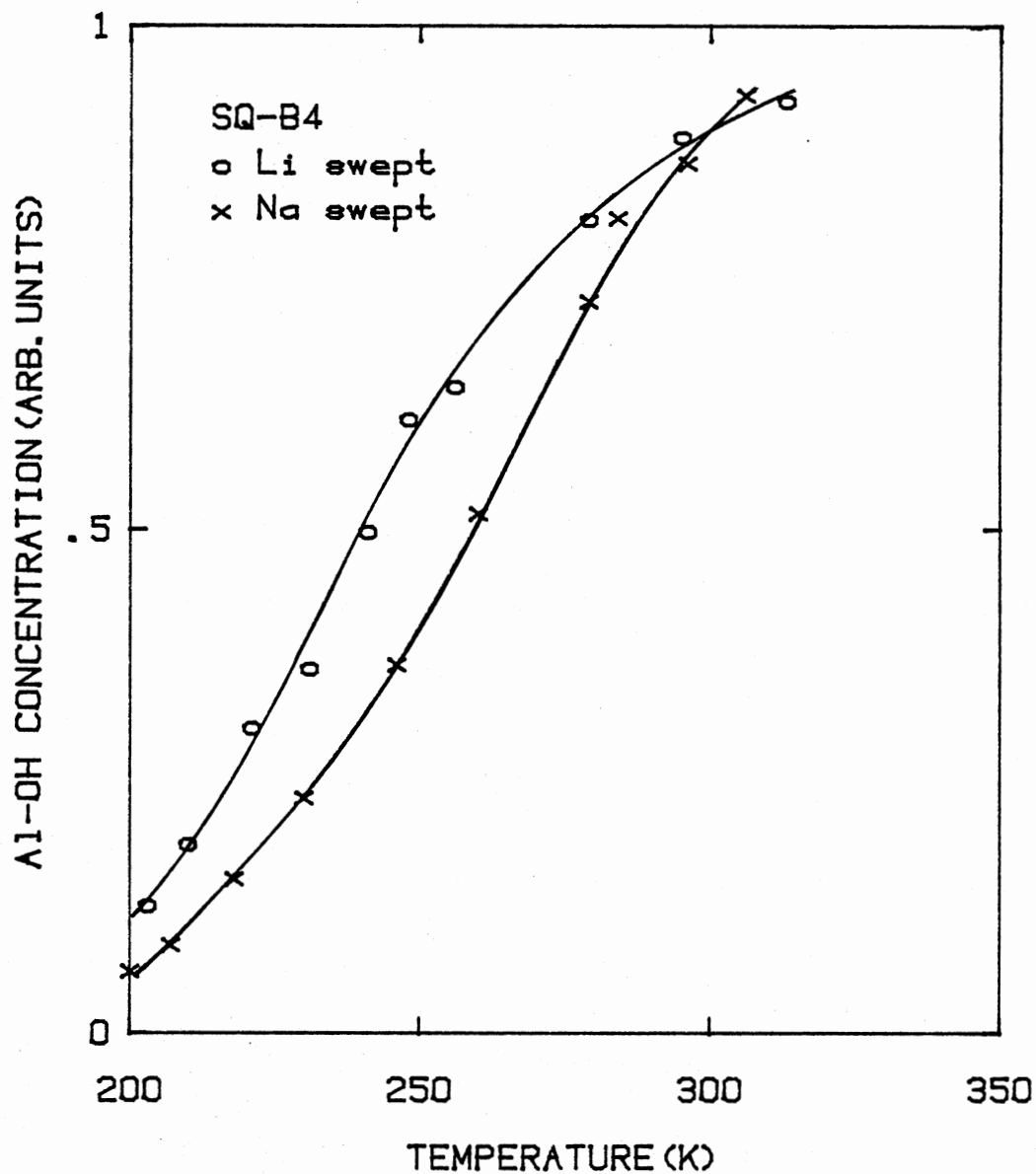


Figure 8. The Concentration of Al-OH Centers as a Function of Irradiation Temperature for Irradiations Performed on the Same Sample While in the Lithium-Swept (As-Received) and Sodium-Swept Conditions. The Concentration is Normalized to One for Each Condition

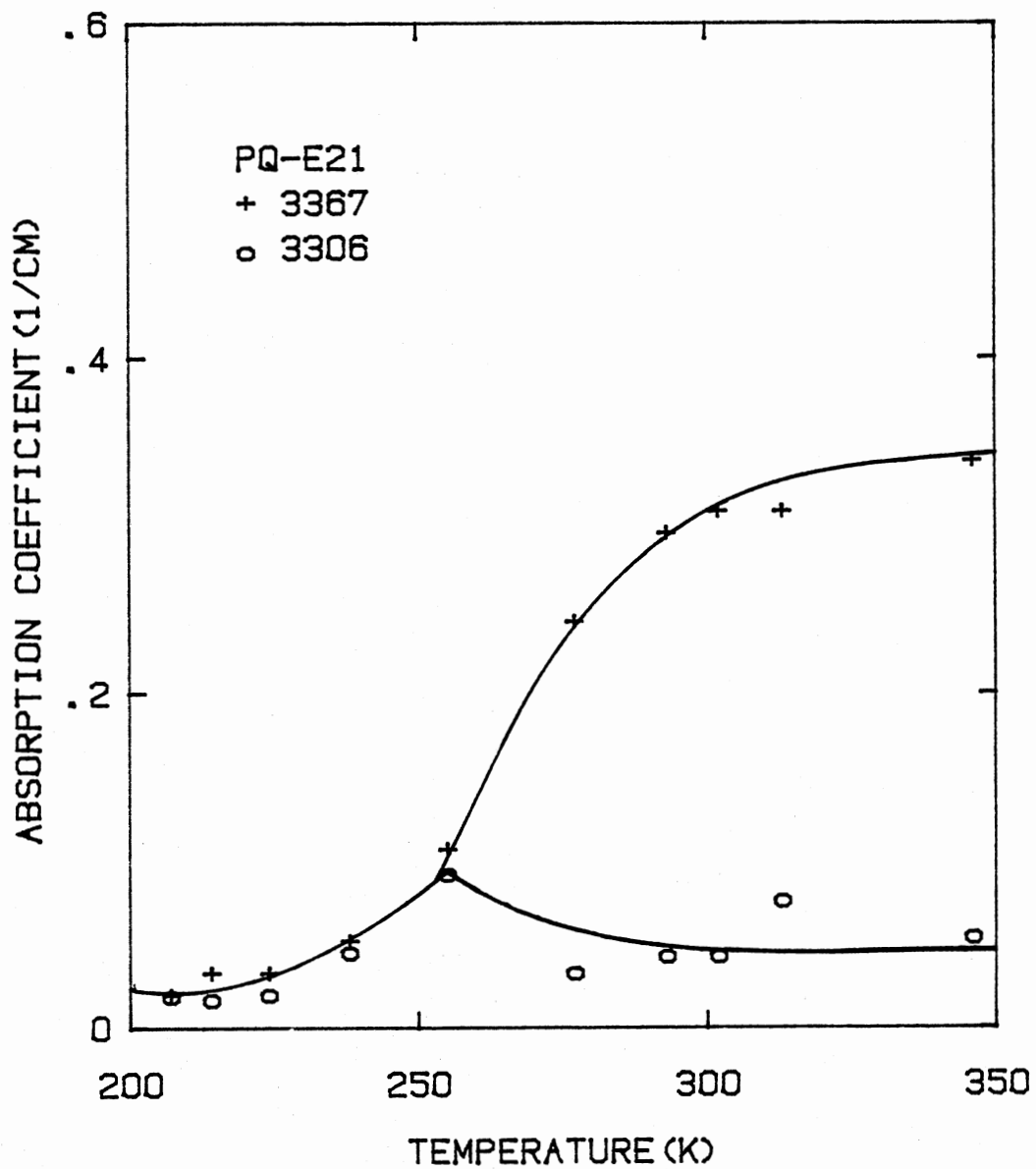


Figure 9. The Growth of  $\text{Al-OH}^-$  Infrared Absorption Peaks as a Function of Irradiation Temperature

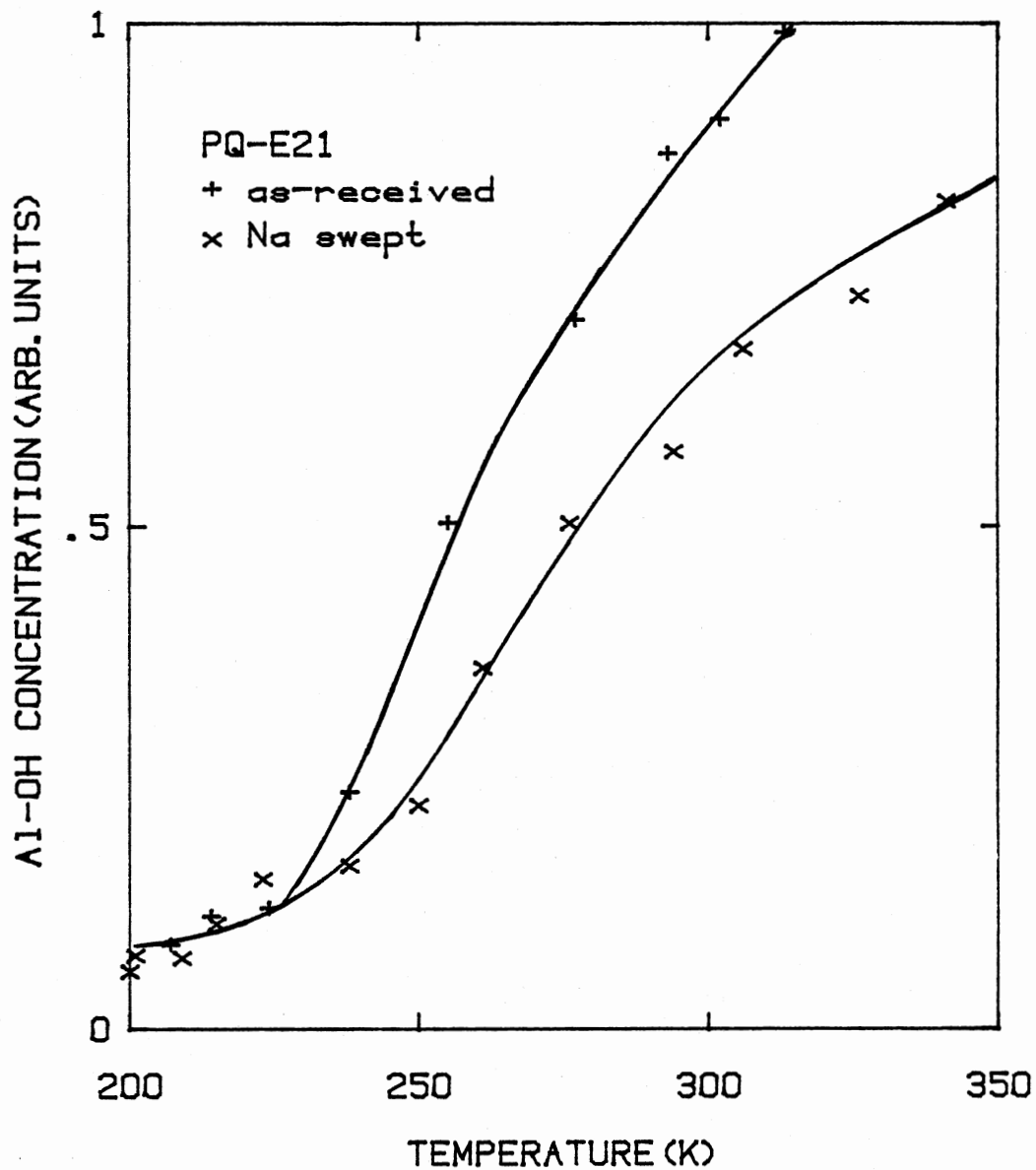


Figure 10. The Concentration of Al-OH Centers as a Function of Irradiation Temperature for Irradiations Performed on the Same Sample While in the As-Received and Sodium Swept Conditions. The Concentration is Normalized to the As-Received Condition

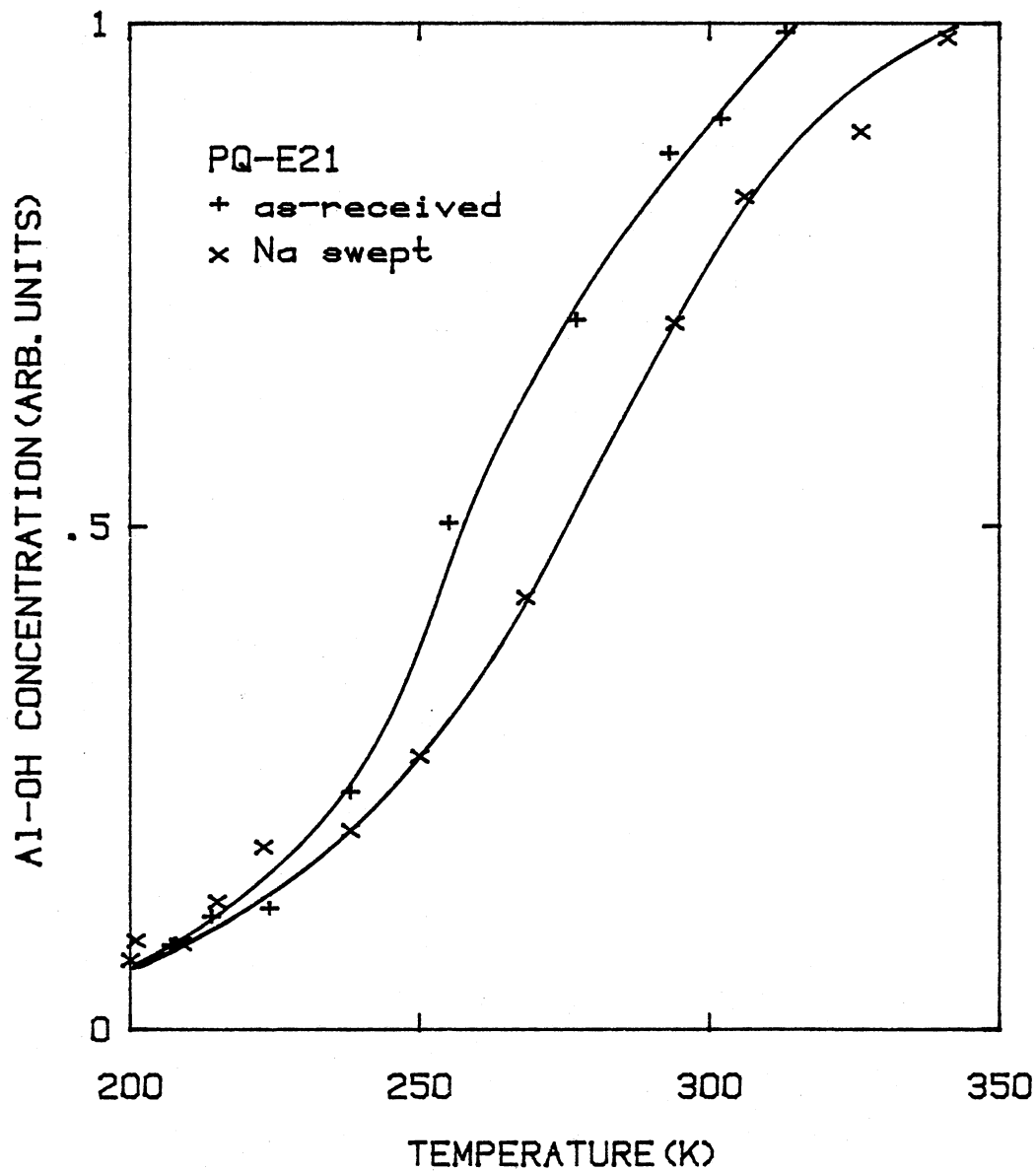


Figure 11. The Concentration of Al-OH<sup>-</sup> Centers as a Function of Irradiation Temperature for Irradiations Performed on the Same Sample While in the As-Received and Sodium Swept Conditions. The Concentration is Normalized to One for Each Condition

## CHAPTER IV

### CONCLUSIONS

Sibley et al. (12) found that the radiation-induced growth of Al-OH<sup>-</sup> centers started at about 200K with saturation occurring around 300K. In the present study, it is found that this growth is dependent on the alkali species present at the aluminum site. On samples which had been Na<sup>+</sup>-swept there is an upward shift relative to Li<sup>+</sup> swept or as-received samples. This shift, of approximately 15K, can probably be accorded to the greater mass and ionic radius which Na possesses with respect to Li. Further it has been noted that the alkali can affect the saturation level of Al-OH<sup>-</sup> centers. For Na<sup>+</sup>-swept samples, there is a significant lowering of the Al-OH<sup>-</sup> saturation level, with respect to Li<sup>+</sup>-swept or as-received samples. This level difference, which can possibly be attributed to a larger production of holes, is as of yet not understood.

## REFERENCES

- (1) IEEE Standard on Piezoelectricity (1978). ANSI/IEEE Std. 1976-1978. Published by the Institute of Electrical and Electronic Engineers, Inc., 345 East 47th Street, New York, New York 10017.
- (2) Kinloch, R. (Private Communication).
- (3) King, J. C., A. A. Ballman and R. A. Laudise. J. Phys. Chem. Solids 23, 1019 (1962).
- (4) Armington, A. F., A. Kahan and F. K. Euler. ETS Technical Memorandum No. 3, Solid State Division, Deputy for Electronic Technology, RADC, Hanscomb AFB, Mass. 01731, September, 1976.
- (5) Halliburton, L. E., N. Koumvakalis, M. E. Markes and J. J. Martin. J. Appl. Phys. 52, 3565 (1981).
- (6) Martin, J. J. (Private Communication).
- (7) King, J. C. Bell Syst. Tech. J. 38, 573 (1959).
- (8) Fraser, D. B. J. Appl. Phys. 35, 2913 (1964).
- (9) Fraser, D. B. Physical Acoustics, Vol. 5, W. P. Mason Ed. (Academic Press, New York, 1968), p. 59.
- (10) Park, D. S. and A. S. Nowick. Phys. Stat. Sol. (a) 26, 617 (1974).
- (11) Martin, J. J., L. E. Halliburton and R. B. Bossoli. Proceedings of the 35th Annual Symposium on Frequency Control, U.S. Army Electronics Command, Fort Monmouth, N. J., pp. 317-320 (1981). Copies available from Electronics Industries Assoc., 2001 Eye St., N. W., Washington, D. C. 20006.
- (12) Sibley, W. A., J. J. Martin, M. C. Wintersgill and J. D. Brown. J. Appl. Phys. 50, 5449 (1979).
- (13) Kats, A. Phillips Res. Rep., 17, 133 (1962).
- (14) Brown, R. N. and A. Kahan. J. Phys. Chem. Solids 36, 467 (1975).

- (15) Griffiths, J. H. E., J. Owen and I. M. Ward. Report of the Bristol Conference--Defects in Crystalline Solids (The Physical Society, London), p. 81 (1955).
- (16) Koumvakalis, N. J. Appl. Phys. 51, 5228 (1980).
- (17) King, J. C. and H. H. Sander. IEEE Trans. Nucl. Sci. NS-19, 23 (1972).
- (18) O'Brien, M. C. M. Proc. Roy. Soc. (London), A231, 404 (1955).
- (19) Weil, J. A. Radiat. Eff. 26, 261 (1975).
- (20) Markes, M. E. and L. E. Halliburton. J. Appl. Phys. 50, 8172 (1979).
- (21) Doherty, S. P. and J. J. Martin. J. Appl. Phys. 51, 4164 (1980).
- (22) Jones, C. K. and C. S. Brown. Proc. Phys. Soc. (London) 79, 930 (1962).
- (23) Sawyer Research Products Inc., 35400 Lakeland Blvd., Eastlake, Ohio 44094.
- (24) Toyo Communications Equipment Company, Kawasaki, Japan.
- (25) Lipson, H. G., F. Euler and A. F. Armington. Proceedings of the Thirty-Second Annual Symposium on Frequency Control, 11 (1978). Copies available from the Electronics Industries Association, 2001 Eye Street, N. W., Washington, D. C. 20006.
- (26) Lipson, H. G., F. Euler and P. A. Ligor. Proceedings of the Thirty-Third Annual Symposium on Frequency Control, 12 (1979). Copies available from the Electronic Industries Association, 2001 Eye Street, N. W., Washington, D. C. 20006.



APPENDIX A

TEMPERATURE VARIATIONS DURING IRRADIATION FOR

SAMPLE SQ-B4 Na SWEEP #1

Temperature Average (K)	Temperature Before (K)	Temperature After (K)	Variation (K)
80	78 78	82 82	$\pm 2$
147	142 141	150 152	$\pm 5$
168	164 164	171 172	$\pm 4$
200	198 199	201 201	$\pm 2$
207	204 203	208 210	$\pm 4$
218	214 213	221 223	$\pm 5$
230	226 226	233 234	$\pm 4$
239	235 235	243 243	$\pm 4$
246	243 243	249 249	$\pm 3$
260	257 257	264 264	$\pm 4$
279	275 278	279 282	$\pm 4$
284	283 282	286 285	$\pm 2$
296	294 294	297 297	$\pm 2$
306	303 305	307 308	$\pm 3$
324	323 324	327 326	$\pm 2$

APPENDIX B

TABULATION OF IRRADIATION DATA

## Sample SQ-B4

Temperature (K)	$\alpha$ (3306) (1/cm)	$\alpha$ (3367) (1/cm)	$\alpha$ Total (1/cm)
as-received			
80	0	.008	.008
156	.008	0	.008
173	0	.015	.015
201	0	.008	.008
211	.029	.045	.074
221	.060	.060	.120
227	.068	.091	.159
230	.091	.106	.197
240	.113	.136	.249
249	.139	.151	.290
259	.169	.211	.380
283	.045	.423	.468
293	.060	.453	.513
307	.060	.483	.543
321	.059	.498	.557

## Na Sweep #1

80	0	.002	.002
147	0	.002	.002
168	.015	.002	.017
200	.011	.015	.026
207	.008	.030	.038
218	.030	.038	.068
230	.045	.060	.105
239	.068	.106	.174
246	.068	.098	.166
260	.076	.159	.235
279	.045	.287	.332
284	.045	.325	.370
296	.048	.347	.395
306	.048	.378	.426
324	.045	.415	.460

## Na Sweep #2

80	0	0	0
170	0	.008	.008
176	0	.008	.008
204	0	.023	.023
212	.016	.033	.049
217	.033	.045	.078
228	.045	.060	.105
236	.064	.079	.143
249	.106	.113	.219
256	.098	.136	.234

Temperature (K)	$\alpha$ (3306) (1/cm)	$\alpha$ (3367) (1/cm)	$\alpha$ Total (1/cm)
279	.038	.272	.310
286	.038	.325	.363
299	.045	.355	.400
310	.042	.378	.420
316	.045	.393	.438
338	.060	.408	.468

## Li Sweep

80	0	.015	.015
175	0	.015	.015
199	0	.030	.030
203	.030	.038	.068
210	.057	.045	.102
221	.076	.091	.167
231	.094	.106	.200
241	.140	.136	.276
248	.153	.186	.339
256	.143	.214	.357
279	.050	.400	.450
295	.063	.433	.496
313	.060	.456	.516
341	.072	.489	.561

## as-Received

80	0	.007	.007
183	.007	.007	.014
199	.013	.017	.030
207	.015	.013	.028
214	.013	.026	.039
224	.016	.026	.042
238	.041	.045	.086
255	.088	.100	.188
277	.029	.236	.265
293	.039	.289	.328
302	.039	.302	.341
313	.072	.302	.375
346	.050	.332	.382

## Na Sweep

85	.007	0	.007
200	.020	0	.020
201	.013	.013	.026
209	.016	.009	.025
215	.018	.020	.038
223	.031	.024	.055
238	.022	.038	.060
250	.031	.052	.083

Temperature (K)	$\alpha$ (3306) (1/cm)	$\alpha$ (3367) (1/cm)	$\alpha$ Total (1/cm)
269	.054	.081	.135
276	.026	.164	.190
294	.020	.197	.217
306	.039	.217	.256
326	.046	.230	.276
341	.050	.262	.312

VITA<sup>2</sup>

Kenneth Barry Hitt

Candidate for the Degree of

Master of Science

Thesis: RADIATION INDUCED MOBILITY OF ALKALI ELECTROLIZED SYNTHETIC QUARTZ

Major Field: Physics

Biographical:

Personal Data: Born in Jonesboro, Arkansas, April 8, 1958, the son of Levi and Maurice Hitt.

Education: Graduated from Jonesboro High School, Jonesboro, Arkansas, in 1976; received Bachelor of Science degree in 1980 from Arkansas State University; completed the requirements for the degree of Master of Science at Oklahoma State University, Stillwater, Oklahoma, in July, 1982.